coatings

MDPI

Article

Combinatorial Sampling and Wear Behavior of Cr-Al-C-N Coatings Deposited by HiPIMS

Joern Kohlscheen

Kennametal GmbH, Altweiherstr. 27-31, 91320 Ebermannstadt, Germany; joern.kohlscheen@kennametal.com

Highlights

What are main findings?

- Combinatorial coating deposition is an effective method to sample Cr-Al nitrides and carbonitrides, and the Cr:Al ratio does not depend significantly on the C:N ratio (when adding two reactive gases).
- Carbon contents at or below 10 atomic % in CrAlCN will increase hardness over that of CrAlN, but only up to a Cr:Al ratio of 1:1 instead of 1:2 (without acetylene reactive gas).
- The modulus is more sensitive to phase formation and decreases steadily below 400 GPa with diminishing Cr content.

What are the implications of the main findings?

- Carbon can replace N in the sublattice; metal sublattice Cr/Al not affected within the measurement error.
- Carbon addition reduces the stability of the hard cubic Cr(Al)N phase at higher Al contents, resulting in a trade-off between desirable Al and C contents.
- Lower acetylene flows to achieve carbon contents of 1–10 atomic % need to be sampled to maintain a high modulus and further minimize tool wear.

Abstract

CrAlN PVD coatings are frequently used to protect cutting tools because of their superior hardness and wear resistance. However, the influence of carbon addition to such coatings remains largely unexplored. Therefore, Cr-Al-C-N coatings were deposited by HiPIMS using a commercial PVD unit equipped with a segmented sputter target. The target consisted of an upper half of Cr and a lower half of Al. Carbon was added under reactive sputtering conditions with the aim of reducing internal stress and introducing a friction-reducing component. A range of different Al-Cr-C compositions could be efficiently explored by varying the acetylene reactive gas flow. Depending on the positioning of the samples, Cr/Al ratios could be varied between about 4/1 and 1/2 while three different levels of carbon concentration (0, 11, and 25 atomic % of total coating composition) were investigated. It was found that an intermediate carbon concentration effectively increased the hardness of Cr-rich coatings, achieving maximum plastic hardness values over 40 GPa. With increasing Al content, hardness drops to below 30 GPa. The cubic CrN phase with mostly 200-oriented grains was detected for most variants. With increasing Al and C contents, a rapid decrease in crystallite size is observed, accompanied by a reduced intensity of the (200) XRD reflection. A turning test on stainless steel showed decreasing flank wear with higher Al contents. However, no improvement associated with carbon addition could be confirmed within the investigated concentration range.

Check for updates

Academic Editor: Luis Cunha

Received: 12 June 2026
Revised: 4 August 2026
Accepted: 5 August 2026
Published: 18 August 2026

Copyright: © 2026 by the author. Licensee MDPI, Basel, Switzerland. This article is an open access article distributed under the terms and conditions of the Creative Commons Attribution (CC BY) license.

Keywords: PVD; HiPIMS; CrAlCN; wear mechanisms; metal cutting

1. Introduction

CrN and CrAlN hard coatings are of interest to the cutting tool and other industries due to their high hardness and ability to form protective oxides [1–3]. It is well known that adding aluminum to CrN is an effective way to improve hardness as long as the cubic phase is preserved. This is normally the case up to an Al content of about 70 at.% (30 at.% Cr) [4,5]. The situation is very similar to that of closely related Ti-Al-N ternary system. The addition of carbon to both CrN or CrAlN offers the possibility to further enhance coating properties, especially when corrosion and friction occur [6–8]. As carbon is of a similar atomic size to nitrogen, it can easily replace it in the cubic lattice and will cause an increase in stress and hardness [9]. However, in contrast to nitrogen, carbon will eventually precipitate as graphite and substantially decrease hardness, and hence, resistance to abrasion [9,10]. Tang et al. varied the carbon content in AlCrCN films deposited by HiPIMS and confirmed an initial hardness increase up to about 5 at.% C, followed by a continuous drop [11]. Interestingly, the authors observed a stronger depletion of Cr, while Al stayed almost constant. It was assumed that mostly CrN bonds were weakened leading to a preferential secondary sputtering of Cr atoms (because of the substrate bias voltage). Tillmann et al. used statistical analysis to optimize CrAlCN coatings for a forming application [12]. It was found that in this case, a high carbon content of around 50 atomic at.% and sufficient hardness (adjusted by a high substrate bias) worked best, although the coatings became quite soft. Romero et al. stated that about 22 at.% of carbon provides the best balance between mechanical and tribological properties in sputtered CrAlCN [8]. While there are numerous tribological studies, few results are available regarding the use of CrAlCN hard coatings for cutting tools [13–15]. As an example, Fang et al. tested AlCrCSiN coatings in dry turning of alloyed steel [13]. Surprisingly, they found that a carbon content of 1 at.% was already enough to reduce flank wear over AlCrSiN. Higher carbon concentrations led to much softer coatings and lower wear resistance. The motivation for this study was hence twofold. First, to make use of the combinatorial deposition approach with the aim of creating several compositions of Cr-Al-C in a single deposition process. Second, to understand and define a suitable range of coating properties for machining ferrous alloys that tend to stick to the cutting tool (such as austenitic stainless steel). A combination of abrasive and adhesive wear components is typically present in this machining application. so adjusting the right amount of carbon for a good balance between hardness and friction behavior will help to optimize tool life.

2. Description of Experiments

All coatings were deposited in an industrial PVD furnace (Cemecon, Wuerselen, Germany) equipped with one rectangular segmented sputter target of 500 mm in height and 88 mm width. The upper half of this target consisted of Cr, while the lower half was made of Al, both metals with a purity of 99.95%, (Avaluxe, Fuerth, Germany). Five samples were placed on a rod in front of the segmented target. The vertical arrangement and step size are shown in Figure 1. The samples consisted of cemented carbide grade K313, ISO K05 (Kennametal, Orwell, OH, USA), style CNMG120408, for analytics and machining tests. Sample 3 was positioned right in front of the intersection of Cr and Al (defined as 0 mm). Positive values indicate positions above, and negative values below, this intersection, as described earlier [16]. As this is an industrial deposition unit, samples rotated on spindles with a closest and farthest distance from the target surface of about

100 and 220 mm, respectively. As the sample height is only 4 mm, a gradient in chemical composition (i.e., the Cr/Al ratio) on a given insert is considered negligible (<1 at.%).

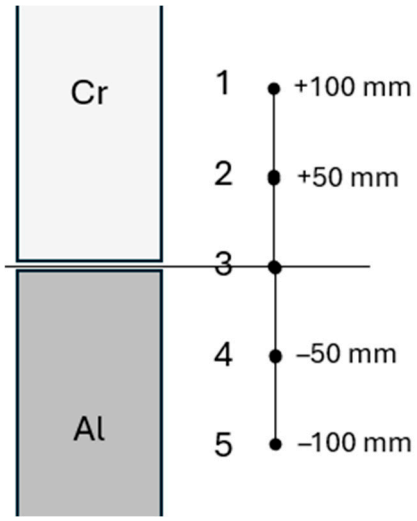


Figure 1. Schematic drawing of sample positions 1–5, vertically aligned in front of the segmented Cr/Al target.

Cleaning was done in an ultrasonically agitated detergent bath for 1 min (T~50 °C), followed by rinsing with ethanol and wiping dry with cleaning paper. The coating process itself consisted of the following steps: evacuation, radiation heating at about 700 °C (60 min), plasma etching (20 min), coating at about 500 °C (120 min), and cooling to 250 °C before opening the coating chamber again. Mid-frequency argon ion etching was performed by applying a ("bias") voltage of 650 V to the substrate table at a frequency of 240 kHz. Important parameters of the HiPIMS deposition process are listed in Table 1. A 10% duty cycle was found to be necessary to ensure a sufficient hardness of the CrAlN coatings. The argon pressure was set to 0.15 Pa (corresponding to about 200 sccm of Ar flow). Nitrogen and acetylene were added at a combined flow of 100 sccm with acetylene flows of 10 and 20 sccm, respectively. An additional set of CrAlN-coated samples was prepared without acetylene reactive gas. Furthermore, DC sputtering was used to prepare reference samples coated with CrAlCN. A monolithic, powder-metallurgical $Cr_{40}Al_{60}$ target (values in atomic %) was used in this case. The DC power was set to 7.5 kW at an acetylene flow of 10 sccm.

Table 1. Overview of main deposition parameters used in HiPIMS deposition of CrAlCN.

Target Power	Pulse Freq.	Pulse-On Time	C_2H_2 Flow	Bias Voltage
7.5 kW	2000 Hz	50 µs (10%)	0/10/20 sccm	100 V

Coating thickness was first determined by a calotte grinding test about 3 mm away from the sample edge. The calotte diameter was measured three times, averaged, and then used to calibrate an X-ray fluorescence (XRF) spectrometer, XDAL (Helmut Fischer, Sindelfingen, Germany). This method is non-destructive and relatively fast, so more thickness data could be captured, leading to improved statistics. Coating adhesion was evaluated by scratch testing using an ST200 instrument (Helmut Fischer). In this method, a diamond stylus (Rockwell C type with a tip radius of 0.2 mm) moves along the surface at an increasing load from 0 to 70 N. Coating failure can be identified in situ by continuous acoustic emissions or by inspecting the scratch using light microscopy after testing.

Elemental concentrations were measured by energy-dispersive X-ray spectroscopy (EDS) with a Phenom XL instrument (ThermoFisher, Waltham, MA, USA). The electron

Helmbeam was accelerated to 15 keV scanning an area of about 130 × 130 µm. While the metals Al and Cr can be determined with an accuracy of about 1 atomic %, the lighter elements typically show increased scatter. Therefore, in this study, any C and N concentrations reported should be considered semi-quantitative and will be verified by more accurate methods in a forthcoming study. However, nitrogen is located next to carbon in the periodic table of elements (with a similar atomic weight and X-ray scattering properties) and showed reasonable values of around 50 at.% in every measurement. Therefore, it is assumed that the values reported for carbon are a good first approximation.

Mechanical properties of the films, such as universal hardness (HM), plastic hardness (H) and reduced modulus (E) were measured by the nanoindentation method using a Fischerscope HM2000 (Helmut Fischer) according to ASTM E 2546. For better accuracy, the coated surface was polished at a slight angle to reduce the scatter of the loading/unloading curves. In order to keep the maximum indentation depth significantly smaller than the film thickness, a load of 10 mN was used without a dwell time at maximum load. This resulted in a typical penetration depth of about 0.1 µm. Twelve indentations were performed on each sample, and the scatter of the results typically stayed around 5% (of the average value).

X-ray analyses were performed with an MF600 unit (Rigaku, Tokyo, Japan) using Cu Kα radiation generated at a voltage of 40 kV and a 20 mA anode current. A Ni K beta filter was used in combination with a Soller slit width of 0.2 mm. An angular range of 30 to 60° was scanned in a Bragg–Brentano setup in order to capture the most intense low-index lattice planes.

The wear resistance (performance) of the different coating variants was evaluated by a turning test on a CNC lathe. A coolant was used to extend tool life. Cutting parameters were set as follows: cutting speed 140 m/min, depth of cut 1 mm, feed 0.2 mm/revolution. An austenitic stainless steel grade EN DIN 1.4301 (Cr-Ni alloyed, corresponding to AISI 304) was used with a tensile strength of close to 600 MPa. Inserts were removed at 2 and 4 min (test end) to visually inspect wear marks on the flank and rake faces. Flank wear progress was measured using light microscopy (VHX system, Keyence, Osaka, Japan). Each test was repeated twice, and the resulting flank wear values were averaged.

3. Results and Discussion

3.1. Thickness and Adhesion

A target thickness of 1.5 µm was intended and could be obtained on average, with some scatter depending on the location of the measured spot. As an example, Table 2 lists values obtained for an acetylene flow of 10 sccm, along with a typical calotte crater image. It is interesting to note that there is a slight trend toward lower thickness from position 1 to 5, which was also found for other experiments. This is most likely caused by a slightly lower sputter yield of Al compared to Cr under irradiation of Ar ions. However, it is assumed that this minor difference in thickness will not significantly affect the machining test results.

Table 2. Coating thickness distribution for an acetylene flow of 10 sccm (all in µm), values determined by XRF, example of calotte used for calibration (right image).

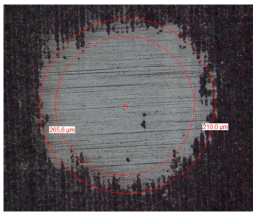
Pos.	Min–Max	Average	
1	1.56–1.80	1.63	
2	1.54–1.80	1.67	
3	1.36–1.60	1.44	
4	1.35–1.61	1.45	
5	1.37–1.59	1.47	

Figure 2 shows images of the scratch track at the end of the test, where a maximum load of 70 N was reached. All coatings without acetylene and with an acetylene flow of 10 sccm passed scratch testing up to 70 N, and no coating delamination was observed at the bottom of the tracks. However, coatings deposited with an acetylene flow of 20 sccm showed delamination for samples at positions 3 to 5, starting at 50 N (pos. 3) and 30 N (pos. 5), respectively, as shown in Figure 2 (right). This reduced adhesion is likely caused by a lack of crystallinity and poor matching to the substrate. The scratch track boundaries are also smoother in Figure 2 (right) indicating softer, more ductile coatings.

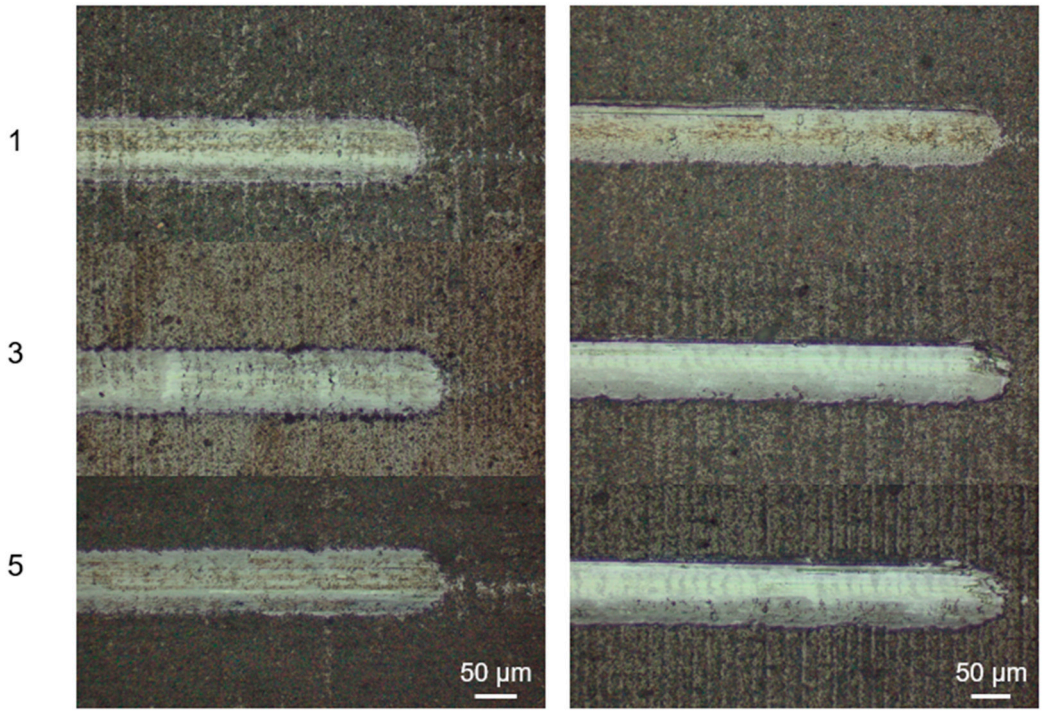


Figure 2. Exemplary images of scratch tracks at maximum load of 70 N, samples of positions 1, 3, 5 with acetylene flows of 10 sccm (**left**) and 20 sccm (**right**).

3.2. Composition, Mechanical Properties, and Structure

One of the main properties of any coating is the concentration of elements present. Table 3 shows trends for the five vertical positions sampled, depending on the flow of acetylene reactive gas. The Cr/Al ratio is expressed as the relative share of Cr in atomic % (metals adding up to 100%) whereas C and N are measured concentrations in atomic % (all elements in the coating adding up to 100%). As expected, moving from position 1 (top) to 5 (bottom), the concentration of Cr drops from about 80 to 30 atomic %. Al is correspondingly increased from about 20 to 70 atomic %. Adding acetylene seems to reduce the amount of Al more than Cr, contradicting the findings of Tang et al. [11]. The reason might be a stronger bonding of Cr-C than Al-C, which would increase the secondary sputtering of Al due to the applied substrate bias voltage.

Table 3. Listing of Cr/(Al+Cr) ratios and concentrations of C, N (in at.%) depending on vertical sample position and acetylene flows (top row, in sccm).

Position	f(Ac) = 0	f(Ac) = 10	f(Ac) = 20
1	0.81/0/52	0.83/11/47	0.82/24/43
2	0.71/0/51	0.74/11/49	0.74/26/44
3	0.55/0/53	0.61/12/50	0.60/24/46
4	0.34/0/54	0.45/12/50	0.48/25/45
5	0.28/0/55	0.32/12/51	0.35/29/45

The deposition with $Cr_{40}Al_{60}$ targets in DC mode and 10 sccm of acetylene reactive gas flow resulted in a Cr/(Al+Cr) ratio of 0.42 and elemental concentrations of 12 (carbon) and 49 (nitrogen) atomic %, respectively. These values are close to the values obtained for the HiPIMS variant deposited with the same amount of acetylene at position 4 at the same flow of acetylene (Table 3).

Figure 3 shows the trends for plastic hardness and elastic modulus for all three variants. The hardness of the CrAlN coatings constantly increases from positions 1 to 5 and saturates at values of almost 45 GPa obtained even for the highest Al content of 72 at.%. Depending on acetylene reactive gas flow, the trends change considerably. For the highest flow of 20 sccm, a constant decrease in hardness is observed, dropping from 35 to about 25 GPa. It can be assumed that Cr-C bonds are diminished when an increasing amount of lattice sites is occupied by Al atoms, which are not known to form equally strong bonds with carbon. The hardness curve for an acetylene flow of 10 sccm reveals the most interesting behavior depending on the sample position. For Cr contents of >50 atomic% (positions 1–3), the hardness is initially increased. Al substitutes Cr in the lattice while carbon does the same for nitrogen atoms; thus, distortion and local stresses go up, which typically results in increased hardness. However, this trend stops at position 4 at a Cr content of <45 atomic % where the softer hexagonal AlN phase is expected to form. Compared to CrAlN, this transition between the cubic and hexagonal phases occurs earlier with carbon present. Zhang et al. reported a similar decrease in hardness but attributed it to graphite precipitation [15]. Interestingly, the DC sputtered variant comparable in composition to the coating at position 4 (acetylene flow of 10 sccm) only shows a hardness of around 25 GPa and a modulus of around 350 GPa. This finding confirms the benefit of the increased ionization obtained with HiPIMS at low duty cycles of around 10%.

The modulus values which are also shown in Figure 3 (bottom diagram) contain further information. Clearly, CrAlN shows higher values overall starting at position 1 with about 450 GPa which increase with higher Al/Cr ratios to over 500 GPa. These high values typically indicate a fully cubic nitride structure. The modulus values for CrAlCN obtained with 10 and 20 sccm of acetylene gas are consistently lower and decline steadily from about 400 to 300 GPa from position 1 to 5. Given the closeness of these curves and their similar dependency on Al concentration, it is assumed that the formation of the hexagonal AlN phase is the main cause of the decreasing modulus values [13].

Figure 4 visualizes x-ray diffraction data of samples taken from positions 1, 3, and 5. The diffraction signal intensity is plotted on a logarithmic scale. Reflections from the carbide substrate remain unchanged in shape and position and serve as reference, i.e., hexagonal WC (100) at 35.7° and cubic Co (111) at 44.2°. The graphs for the CrAlN coatings at the top clearly show a cubic CrN phase with reflections from the (111) and (200) crystal planes around 37.6° and 43.7°, respectively. Transitioning from position 1 to 5 leads to a reduction in peak signal intensity and a shift to larger diffraction angles as Al gradually replaces Cr on its lattice sites. CrAlCN coatings obtained by adding 10 sccm of acetylene reactive gas do not clearly show a signal for the (111) plane. The peak originating from the (200) plane is reduced in intensity and broadened, with the signal becoming fainter from position 1 to 5 (increasing Al concentration). A similar behavior was described by Zhou et al. for arced AlCrCN with increasing acetylene gas flows [10]. The graph at the bottom is a diffraction diagram of a DC-sputtered CrAlCN coating ($Al_{60}Cr_{40}$ targets, acetylene flow of 10 sccm) for comparison. It resembles the graphs obtained for position 5, but additionally seems to indicate the presence of a hexagonal AlN phase (peak at 31.8°, $10\underline{1}0$ plane). Unlike the study by Romero et al. a distinct carbide phase [8] or precipitated carbon could not be detected with the applied methods. X-ray photoelectron spectroscopy [11] or Raman spectroscopy [13] were previously used to study the bonding of carbon in CrAlCN coatings.

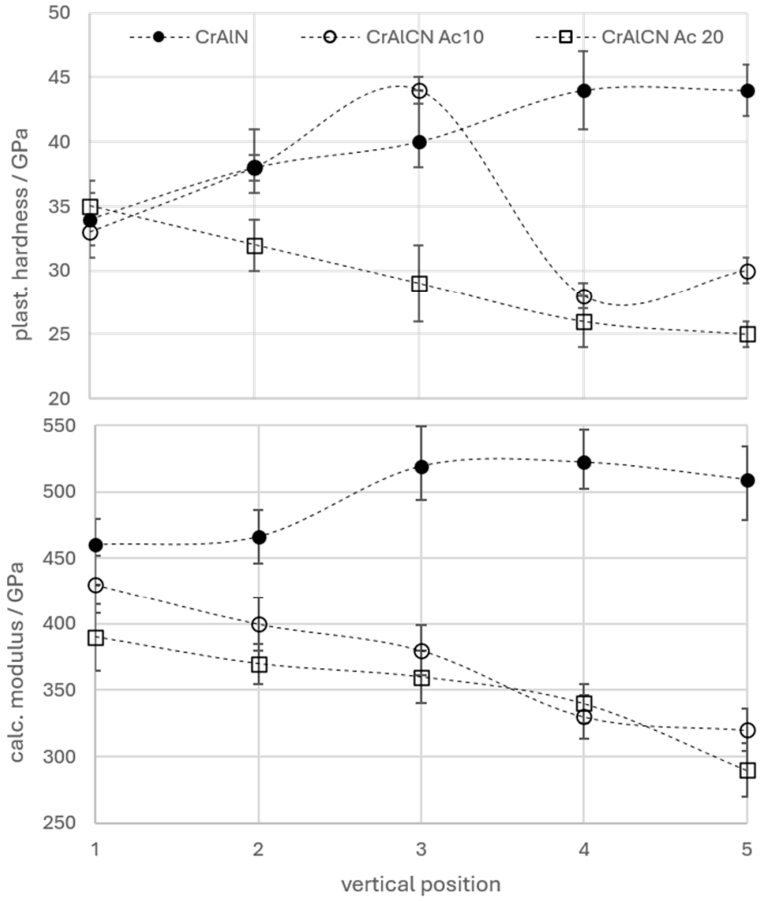


Figure 3. Plastic hardness and modulus depending on vertical position and acetylene gas flow (e.g., "Ac 10" indicates a flow 10 sccm).

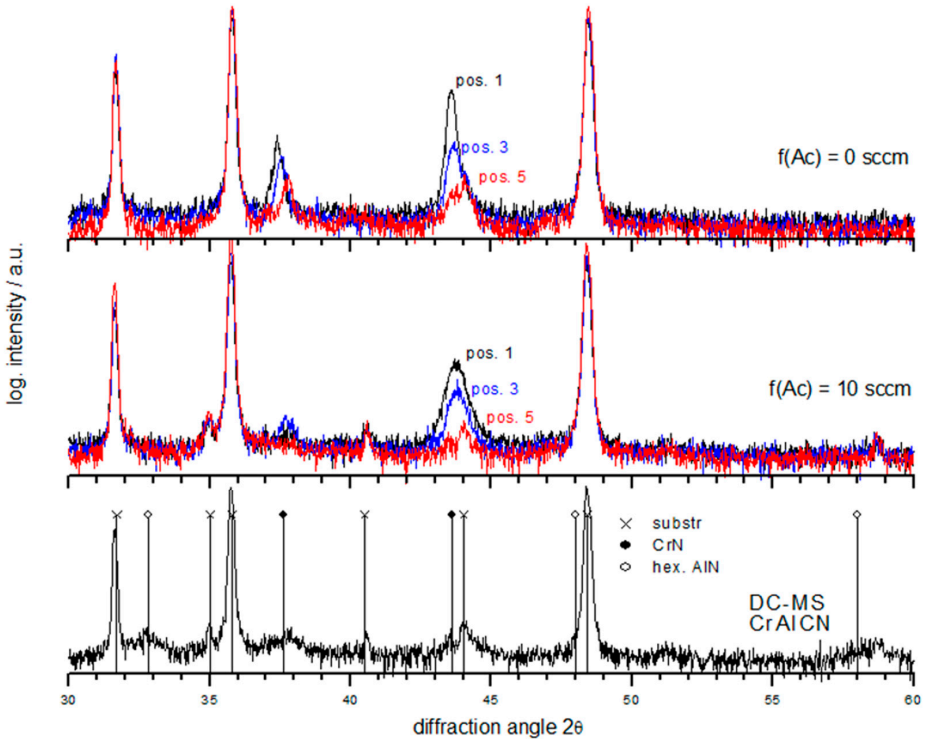


Figure 4. X-ray diffraction diagrams of CrAlCN-coated samples from pos. 1, 3 and 5 deposited without and with acetylene gas flow of 10 sccm (HiPIMS process middle graph, DC process lower graph).

https://doi.org/10.3390/coatings16080984

3.3. Metal Cutting Test

As described in the experimental Section 2, a turning test was done to evaluate the wear behavior of differently coated carbide inserts when machining a material that tends to adhere to the cutting tool. Two batches with the hardest coatings were compared: CrAlN and CrAlCN, deposited with an acetylene flow of 10 sccm which according to Figure 3, were overall significantly harder than the coating variants obtained with a higher reactive gas flow. The relatively soft variants obtained with a higher acetylene gas flow were hence not tested further. Figure 5 shows the resulting flank wear after 4 min of turning stainless steel, together with two exemplary images of the rake face after completing the test; positions 1 (Cr rich) to 5 (Al rich) are again shown. In the case of CrAlN, there is a trend toward reduced flank wear marks with increasing Al content, reaching its lowest value for the highest content of Al. This trend is in accordance with trends in hardness and modulus, so an abrasive wear mechanism is assumed. CrAlCN coatings showed a less clear trend depending on the Cr/Al ratio, and a minimum can be observed at position 4. This finding could be explained by competing effects of increasing hardness and decreasing modulus, which reach an optimum near position 4 at a Cr content of about 45 atomic % (Table 3). In the case of CrAlN, high hardness and modulus values are preserved for Cr content as low as 28 atomic %. Therefore, carbon addition reduces the allowable Al content before hardness and the associated abrasive wear resistance drop. In fact, Fang et al. used $Al_{70}Cr_{30}$ targets and could only add about 2 atomic % carbon before the hardness was reduced notably [13].

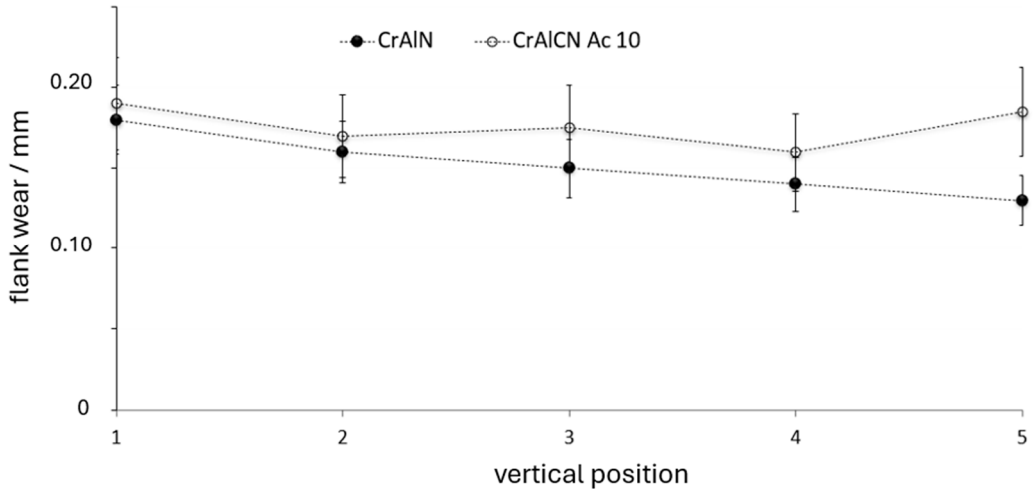


Figure 5. Turning test flank wear after 10 min of continuous turning of AISI 304 depending on sample position, coatings CrAlN and CrAlCN (acetylene gas flow of 10 sccm, "Ac 10").

Finally, Figure 6 shows the rake face of sample position 3 (CrAlN and CrAlCN deposited with an acetylene flow of 10 sccm). The wear observed at these edges appears comparable with clearly visible crater wear (upper brighter area) and workpiece adhesion directly below the curved cutting edge. A qualitative EDS spot measurement (indicated by the '+' sign close to the image center) reveals the presence of the metals Fe, Cr, and Ni in adhered workpiece material in both cases.

It is obvious that wear progresses quite fast under the cutting conditions applied. The substrate material is exposed early, which determines further wear behavior. This makes it difficult to detect significant differences that are caused by differing coating properties. Therefore, further testing is planned using both tribometry and metal cutting (with reduced speed and increased coating thickness).

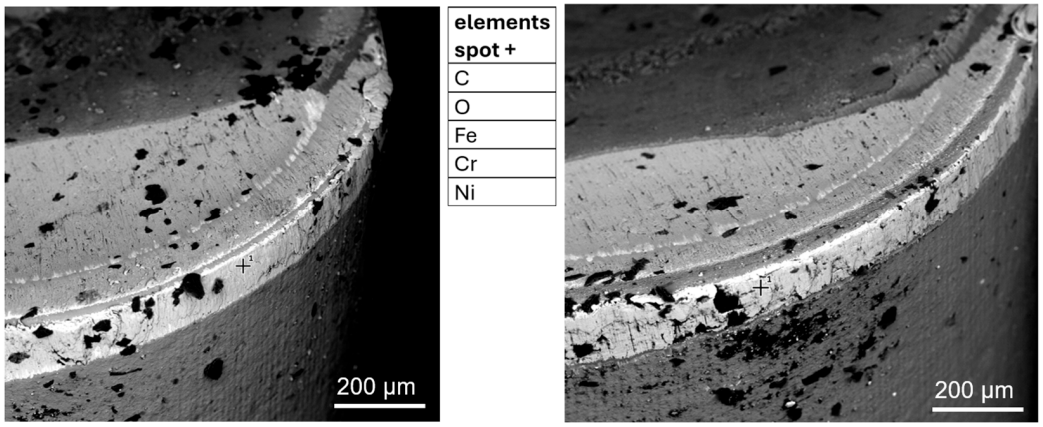


Figure 6. Qualitative EDS of workpiece material adhered to the cutting edge after 4 min of turning, samples of position 3, CrAlN (**left**) and CrAlCN (Ac = 10 sccm, **right**) coatings.

4. Conclusions

CrAlCN thin films were deposited in an industrial-scale HiPIMS PVD unit using a target consisting of Cr and Al metallic segments. This setup allowed several elemental ratios to be sampled in a single coating process. Five vertical positions were chosen in this study. A further variable was explored by adding acetylene to the nitrogen reactive gas. It was found that acetylene is much more effective than nitrogen in poisoning the target surface, likely because it can be ionized more easily due to its relatively weak C-H bonds. The face-centered cubic Cr(Al)N phase was present for all sampled Cr/Al/C ratios. X-ray diffraction showed decreasing signal intensity with increasing Al content and with higher acetylene flows. CrAlN coatings without carbon were already very hard, with a maximum plastic hardness of over 40 GPa at a Cr/Al atomic ratio of about 40/60. By adding about 10 at.% carbon, a comparable peak hardness of over 40 GPa occurred at a lower, roughly equal, Cr/Al elemental ratio. However, the modulus of all carbon-enriched coating variants decreased with increasing Al concentration. The most likely explanation is the formation of the hexagonal AlN phase, which is promoted by an increasing carbon concentration. Coatings deposited with the highest acetylene flow of 20 sccm showed a rapid decline in hardness with increasing Al content and were therefore not considered for wear testing. A turning test on stainless steel did not show an improved tool life for the CrAlCN coatings deposited with an acetylene flow of 10 sccm when compared to the CrAlN coated inserts. The carbide substrate was exposed early on the rake face and the cutting edge in all cases, leading to rapid workpiece adherence. Further testing at less severe cutting conditions, accompanied by tribological studies, is planned in order to better detect the effects of differing coating properties.

Funding: This research received no external funding.

Data Availability Statement: The original contributions presented in this study are included in the article. Further inquiries can be directed to the corresponding author.

Conflicts of Interest: Author Joern Kohlscheen was employed by the company Kennametal GmbH. The author declares that the research was conducted in the absence of any commercial or financial relationships that could be construed as potential conflicts of interest.

References

1. Tillmann, W.; Stangier, D.; Laemmerhirt, I.A.; Biermann, D.; Freiburg, D. Investigation of the tribological properties of high-feed milled structures and Cr-based hard PVD-coatings. *Vacuum* **2016**, *131*, 5–13. [CrossRef]
2. Mo, J.L.; Zhu, M.H.; Leyland, A.; Matthews, A. Impact wear and abrasion resistance of CrN, AlCrN and AlTiN PVD coatings. *Surf. Coat. Technol.* **2013**, *215*, 170–177. [CrossRef]

3. Bagcivan, N.; Bobzin, K.; Theiss, S. ($Cr_{1-x}Al_x$)N: A comparison of direct current, middle frequency pulsed and high power pulsed magnetron sputtering for injection molding components. *Thin Solid Films* **2013**, *528*, 180–186. [CrossRef]
4. Reiter, A.; Derflinger, V.H.; Hanselmann, B.; Bachmann, T.; Sartory, B. Investigation of the properties of $Al_{1-x}Cr_xN$ coatings prepared by cathodic arc evaporation. *Surf. Coat. Technol.* **2005**, *200*, 2114–2122. [CrossRef]
5. Weirather, T.; Czettl, C.; Polcik, P.; Kathrein, M.; Mitterer, C. Industrial-scale deposition of $Cr_{1-x}Al_xN$ coatings with $0.21 < x < 0.74$ from segmented targets. *Surf. Coat. Technol.* **2013**, *232*, 303–310. [CrossRef]
6. Xu, X.; Sun, J.; Xu, Z.; Li, Z.; Su, F. Microstructure, electrochemical and tribocorrosion behaviors of CrCN nanocomposite coating with various carbon contents. *Surf. Coat. Technol.* **2021**, *411*, 126997. [CrossRef]
7. Soleimani, M.; Alhosseini, A.F.; Elmkhah, H.; Babaei, K.; Imantalab, O. A comparison of tribological and corrosion behavior of PVD-deposited CrN/CrAlN and CrCN/CrAlCN nanostructured coatings. *Ceram. Int.* **2023**, *49*, 5029–5041. [CrossRef]
8. Romero, E.C.; Botero, M.G.; Tillmann, W.; Osorio, F.B.; Gaitan, G.B. Influence of carbon content on the microstructure, mechanical and tribological properties of CrAlCN coatings deposited by DC unbalanced magnetron sputtering. *Bull. Mater. Sci.* **2018**, *41*, 97. [CrossRef]
9. Almer, J.; Oden, M.; Hakansson, G. Microstructure, stress and mechanical properties of arc-evaporated Cr-C-N coatings. *Thin Solid Films* **2001**, *385*, 190–197. [CrossRef]
10. Zhou, Q.; Wang, X.; Huang, B.; Chen, Q.; Liang, D.; Zhang, E.; Lou, Z. Investigation of the microstructure, mechanical and tribological properties of CrAlCN composite coatings with various acetylene flow rates. *Thin Solid Films* **2026**, *835*, 140859. [CrossRef]
11. Tang, J.F.; Wang, S.H.; Yang, F.C.; Chang, C.L. Effects of carbon doping and DC bias voltage on microstructure and mechanical properties of AlCrCN films synthesized via HiPIMS. *Materials* **2022**, *15*, 5729. [CrossRef] [PubMed]
12. Tillmann, W.; Stangier, D.; Schröder, P. Investigation and optimization of the tribo-mechanical properties of CrAlCN coatings using Design of Experiments. *Surf. Coat. Technol.* **2016**, *308*, 147–157. [CrossRef]
13. Fang, W.; Chen, J.; Zhou, Q.; Xue, H.; Cai, F.; Fang, L.; Zhang, S. Microstructure, mechanical properties and high speed dry-cutting performance of AlCrSiCN composite coatings. *J. Mater. Res. Technol.* **2023**, *25*, 1800–1812. [CrossRef]
14. Jie, S.; Tian, H.; Li, J.; Zhang, P.; Hong, Z.; An, S. Study on the working performance of CrAlCN coated and uncoated carbide twist drill. *Optik* **2022**, *270*, 169948. [CrossRef]
15. Zhang, M.; Zhou, F.; Fang, H.; Wu, Z. Influence of C content on the structure, mechanical and tribological properties of CrAlCN films in air and water-based cutting fluid. *Appl. Phys. A* **2020**, *126*, 589. [CrossRef]
16. Kohlscheen, J.; Bareiss, C. Combinatorial deposition and wear testing of HiPIMS W-C films. *Coatings* **2025**, *15*, 115. [CrossRef]

Disclaimer/Publisher's Note: The statements, opinions and data contained in all publications are solely those of the individual author(s) and contributor(s) and not of MDPI and/or the editor(s). MDPI and/or the editor(s) disclaim responsibility for any injury to people or property resulting from any ideas, methods, instructions or products referred to in the content.